RESEARCH ARTICLE | JUNE 19 2018

# Kirigami stretchable strain sensors with enhanced piezoelectricity induced by topological electrodes

Rujie Sun; Bing Zhang; Lu Yang; Wenjiao Zhang; Ian Farrow; Fabrizio Scarpa ✉; Jonathan Rossiter ✉



*Appl. Phys. Lett.* 112, 251904 (2018)
https://doi.org/10.1063/1.5025025







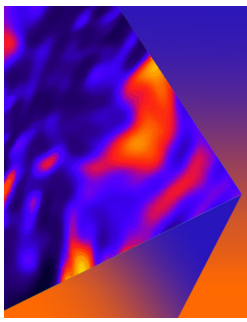

# Kirigami stretchable strain sensors with enhanced piezoelectricity induced by topological electrodes

Rujie Sun,[1] Bing Zhang,[1] Lu Yang,[2] Wenjiao Zhang,[3] Ian Farrow,[1] Fabrizio Scarpa,[1,a)] and Jonathan Rossiter[4,a)]
[1]*Bristol Composites Institute (ACCIS), University of Bristol, Bristol BS8 1TR, United Kingdom*
[2]*College of Mechanics and Materials, Hohai University, Nanjing 210098, China*
[3]*School of Engineering, Northeast Agricultural University, Harbin 150030, China*
[4]*Department of Engineering Mathematics, University of Bristol, Bristol BS8 1UB, United Kingdom*

(Received 6 February 2018; accepted 16 May 2018; published online 19 June 2018)

Rapid advances in sensing technologies are leading to the development of integrated wearable electronics for biomedical applications. Piezoelectric materials have great potential for implantable devices because of their self-powered sensing capacities. The soft and highly deformable surfaces of most tissues in the human body, however, restrict the wide use of piezoelectric materials, which feature low stretchability. Flexible piezoelectric polyvinylidene fluoride films that could conformably integrate with human bodies would have advantages in health monitoring. Here, a Kirigami technique with linear cut patterns has been employed to design a stretchable piezoelectric sensor with enhanced piezoelectricity. A parametric Finite Element Analysis study is first performed to investigate its mechanical behaviour, followed by experiments. An inter-segment electrode connection approach is proposed to further enhance the piezoelectric performance of the sensor. The voltage output shows superior performance with 2.6 times improvement compared to conventionally continuous electrodes. Dynamic tests with a range of frequencies and strains are performed to validate the sensor design. With its high performance in large strain measurements, the Kirigami-based sensing system shows promise in stretchable electronics for biomedical devices. 
https://doi.org/10.1063/1.5025025

Implantable biomedical devices have recently received significant attention from the healthcare industry. However, most implantable electronics are powered by internal batteries whose life-span restricts long term operations. Additional surgery for battery replacement is undesirable due to increased pain and risks to the patients. A sustainable power source derived from the biological system itself is therefore crucial for implantable devices. Piezoelectric materials are viable candidates for such implantable sensing systems, since they can be used as self-powered battery-free sensors with intrinsic mechano-electric energy harvesting ability.[1] Many efforts have been dedicated to the development of piezoelectric sensors for health monitoring, as discussed in recent review papers.[2–4] Two main types of piezoelectric materials are widely used, organic and inorganic. Inorganic piezoelectric materials such as lead zirconate titanate (PZT), zinc oxide (ZnO), and barium titanate (BaTiO3) are quite stiff and brittle in the bulk state, thus not well-suited to flexible biomedical systems directly. Many approaches have been explored to solve this challenge, including the fabrication of thin films[5,6] and nanowires[7,8] from these materials. The aforementioned processes involve expensive and complicated microfabrication and material synthesis techniques, which are not suitable for mass production. Organic materials are preferable for biomedical applications; their natural flexibility enables them to conform to the soft surface of human tissues. Polyvinylidene fluoride (PVDF) and its copolymer poly [(vinylidenefluoride-co-trifluoroethylene) [P(VDF-TrFE)] are two of the most commonly used organic piezoelectric materials, and have shown promise for biomedical applications due to their outstanding piezoelectric characteristics, mechanical ductility, and biocompatible properties.[9]

Extensive studies have been performed to improve the piezoelectric properties by facilitating the formation of $\beta$ phase crystals. This can be achieved by incorporating particles, such as ferrite nanoparticles,[10] carbon nanotubes,[11] and hybrid nanocomposites,[12] into the polymer matrix. A mesoporous PVDF film with ZnO nanoparticles as the sacrificial template represents an innovative method to induce the formation of the $\beta$ phase due to the interactions between PVDF dipoles and the ZnO surface.[13] Such an implantable piezoelectric device exhibits outstanding performances *in vivo*, and it is also fully compatible with the biological environment.[9] Surface morphology also plays a key role in elevating the power output, and a smooth and flat surface of the P(VDF-TrFE) film results in an eight-fold increase in voltage output over a rough surface.[1]

In addition to high sensitivity, a health monitoring system also requires high stretchability to offer 3D shape changing within the human body. However, traditional PVDF films show extremely low stretchability, thus limiting their applications in implantable devices. Recently, the Kirigami approach, the Japanese art of cutting and folding paper, has been proven to be a versatile technology to design diverse mechanical metamaterials with multiple functionalities.[14,15]

a)Authors to whom correspondence should be addressed: F.Scarpa@bristol.ac.uk and Jonathan.Rossiter@bristol.ac.uk

 

The mechanical properties of a Kirigami structure can be tuned and programmed based on a tailored pattern of cuts. For example, a hierarchical fractal cut is demonstrated to be an effective method to design highly stretchable metamaterials.[16–18] Unit cut geometry and hierarchical levers are two important parameters that determine the mechanical behavior. Moreover, the sheet thickness significantly affects the transition from in-plane deformation to out-of-plane deformation, and a thin sheet is prone to trigger mechanical instabilities with induced buckling, forming a variety of three dimensional (3D) architectures.[19–22] The Kirigami approach effectively broadens the design possibilities for a wide range of flexible materials, with the length scale spanning from nanometers to centimeters. The remarkable features of Kirigami structures have recently been introduced in a variety of applications. To improve the power generation of flat solar cells, a simple linear cut pattern is made into thin films of gallium arsenide, and the angle of the tilted panel can be controlled by the stretching strain in order to track the Sun's position.[23] With a similar Kirigami pattern, the stretchability of nanocomposite based conductors has been improved from 2% to beyond 100%, with stable conductivity.[24,25] By introducing different functional materials, a variety of applications have been achieved, such as stretchable graphene transistors,[26] mechanical actuators,[26,27] stretchable batteries,[28] supercapacitors,[29] and deployable reflectors.[30,31] A recent study has shown ultrastrechable bioprobes with a Young's modulus of 3.6 KPa and a stretchability of 840%, which could intimately follow the shape changes of biological tissues. *In vivo* tests demonstrate that this Kirigami based device could record the electrocardiogram signals of a beating mouse's heart whose volume and surface area experience large and rapid changes.[32] This work has validated the potentials of the Kirigami approach in biomedical applications.

Here, we propose a Kirigami piezoelectric sensor with high stretchability and enhanced piezoelectricity. Combined numerical and experimental results demonstrate that tunable and programmable mechanical behavior can be achieved by adjusting the geometric parameters of the cut patterns. We have then fabricated a piezoelectric sensor by making a linear cut pattern into a thin PVDF film. To enhance the electric performance, an inter-segment electrode design is explored through Finite Element Analysis (FEA) and experiments. Finally, dynamic tests at various frequencies and tensile strain levels have been performed on the stretchable piezoelectric sensor system.

The patterns of cuts in the Kirigami structure need to be algorithmically designed to obtain a specific mechanical performance. We use here a simple and effective linear pattern of cuts in a thin flat film, forming the Kirigami structure of Fig. 1(a). To understand the overall mechanical deformation

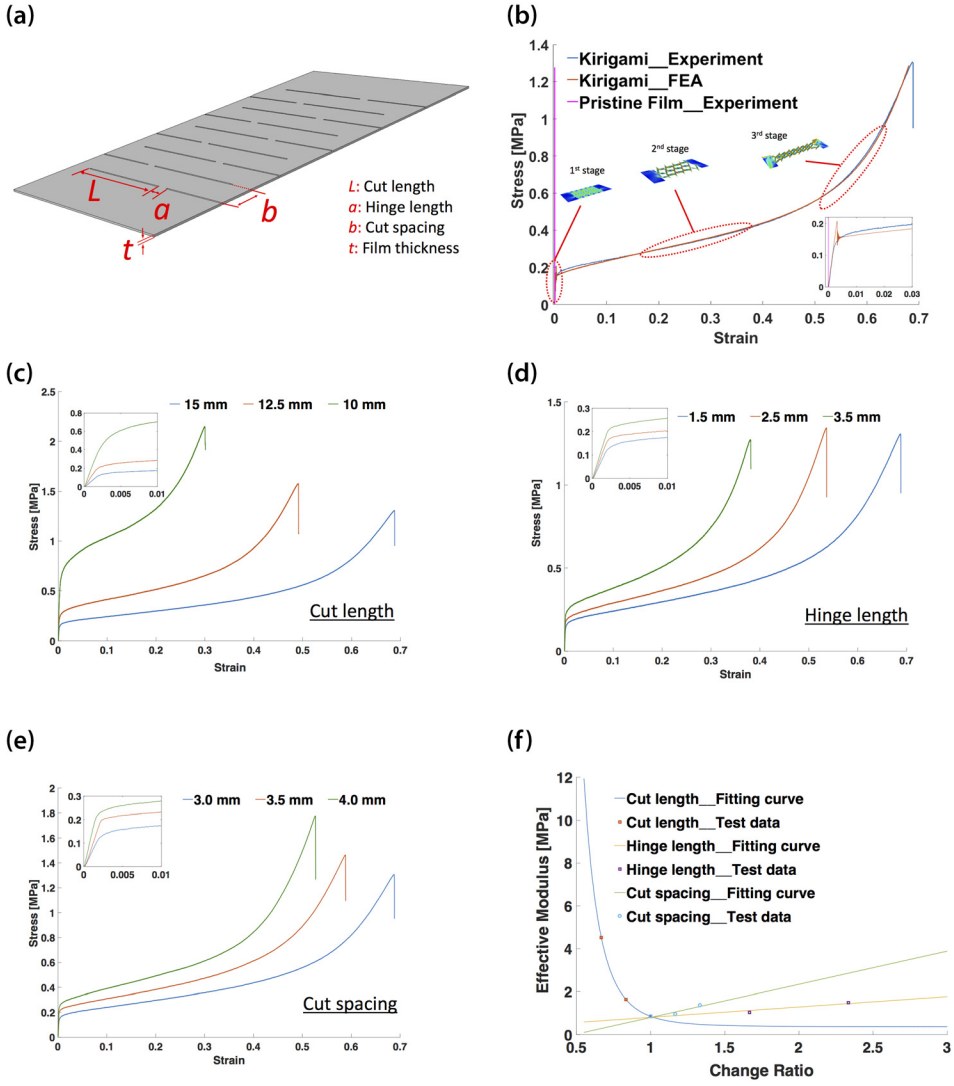


FIG. 1. (a) Schematic of the Kirigami structure where $L$, $a$, $b$, and $t$ indicate the cut length, hinge length, cut spacing, and film thickness. (b) Stress-strain curves for the pristine film, and the Kirigami patterned film obtained by numerical simulations and experiments; experimentally obtained stress-strain curves by varying a single geometric parameter, including the cut length in (c), the hinge length in (d), and the cut spacing in (e), where the control Kirigami parameters are $L = 15$ mm, $a = 1.5$ mm, and $b = 3$ mm, respectively; (f) summary of the dependence of effective modulus on the geometric parameters, where the change ratio indicates the normalized value of each parameter relative to its control value.

of the Kirigami configurations, thin polyethylene terephthalate (PET) films with this linear pattern are analyzed. A uniaxial tensile test was performed on the structure with one end clamped and the tensile loading introduced via the other end. FEA (see supplementary material) was also used to analyze the stress-strain response of the Kirigami structure. The FEA predictions correlate very well with the experimental measurements [Fig. 1(b)]. The typical stress-strain curves of the Kirigami structure show three different stages. During the first stage, the structure undergoes an initial elastic deformation which is restricted within the in-plane stretching. The effective stiffness of the structure is governed by the in-plane bending of the hinges. Once the applied force reaches the critical buckling load, a mechanical instability is triggered, with a transition from in-plane deformation to out-of-plane buckling (second stage). The out-of-plane bending and rotation of the cut strips lead to a moderate stress growth within a high strain, thus enhancing the stretchability. The third stage occurs with further loading, and the subsequent deformation mode switches from bending back to stretching again. Stress concentration is localized in the edge of the cuts, leading to a sharp increase in the effective stiffness, and finally to fracture.

Analytical studies have been performed on a range of linear cut patterns, showing that there are several geometric parameters and material properties that determine the mechanical behavior of this type of Kirigami structures. The fundamental parameters are the cut length $L$, the hinge length $a$, the spacing between the cuts $b$, the film thickness $t$, and the Young's modulus $E$ of the underlying material.[20] The effective modulus of the whole structure is a key emergent metric to be evaluated through a parametric exploration. For biomedical devices, a low effective modulus would be preferable to enable an adaptation to the deformation of the tissue. We carried out a series of experiments with different geometric parameters to characterize the mechanical response. The effective modulus is calculated from the ratio between the nominal stresses and strains within a 0.5%–10% strain range to avoid the nonlinear buckling effect of the initial stage. The modulus is adopted as the indicator for the comparison. The results from Figs. 1(c) to 1(e) show that the effective modulus could be readily tuned by controlling the geometric parameters. An increase in the cut length $L$ would soften the structure with a low effective modulus. Increasing the hinge length $a$ and the cut spacing $b$ would make the structure more rigid, leading to a higher effective modulus. From Fig. 1(f), it can be seen that the cut length has an exponential effect on the mechanical behavior, while the other parameters exhibit a linear relationship with the effective modulus. These parametric studies were also performed by FEA, and the general trends shown in experiments are replicated in FEA as well (see supplementary material). The strain at failure is also an important factor for sensor design, and the relation between the limit strain and the geometric parameters based on the test data is summarized in Fig. S3.

We then introduce the linear Kirigami cut pattern into a thin PVDF film to design a stretchable piezoelectric strain sensor. A FEA study was first performed to optimize the electrode design of the Kirigami piezoelectric sensors. As seen in Fig. 2(a), for the wavy unit of the Kirigami structure, the local strain distribution along its neutral axis is variable, with compression in blue areas and tension in red areas coexisting on the same surface. If the Kirigami pattern is directly introduced into the PVDF film with a continuous electrode, a charge cancellation would occur due to the opposite strain distribution on the same side of the electrodes. An inter-segment electrode pattern is therefore proposed to improve the electric performance.[33] Rather than using a continuous electrode over the surface, we use only a segment corresponding to one quarter of the wavelength of the buckled section, and located in the highest strain region [Fig. 2(b)]. Then, the opposite electrodes between segments are reversely connected through holes [Fig. 2(b)]. In order to validate the proposed inter-segment connection

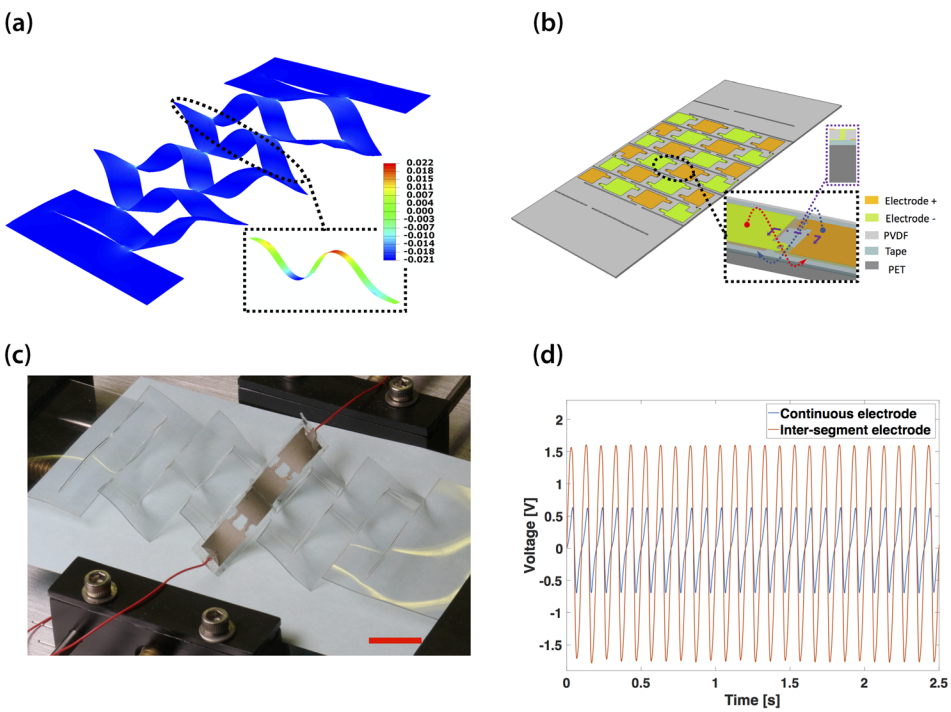


FIG. 2. (a) The FEA of the mechanical response of the Kirigami structure. The inset is the local strain distribution on a unit strip. (b) The inter-segment electrode pattern with reverse connections for adjacent parts through holes. (c) The electrode pattern using inter-segment connections within one unit strip of the Kirigami structures, scale bar 2 cm. (d) The time domain output of voltage using the electrode patterns in (c) from experimental tests.

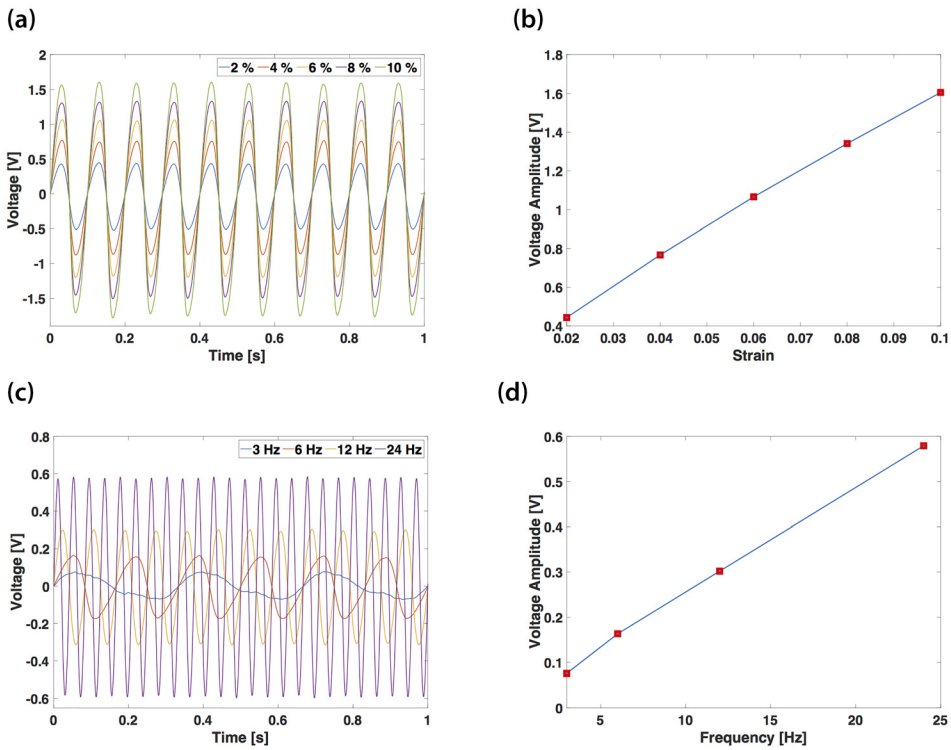


FIG. 3. (a) Voltage output of the Kirigami piezoelectric sensor under a given frequency of 10 Hz and a strain range from 2% to 10% and (b) the effective sensitivity; (c) the voltage output under a given strain range of 1% and a frequency range from 3 Hz to 24 Hz, and (d) a corresponding plot of amplitude versus frequency.

mechanism, an experimental comparative study was performed between the proposed design and the conventional continuous configuration [Figs. 2(c) and 2(d)]. The Kirigami-based piezoelectric sensor has a two-layer topology, with a 125 $\mu$m thickness of PET film as the substrate and a 28 $\mu$m thickness of the PVDF film. The parameters of the cut patterns are: cut length $L = 22.5$ mm, hinge length $a = 2.25$ mm, and spacing between cuts $b = 8.25$ mm. Kirigami based piezoelectric sensors with these two electrode designs were fabricated with one strip of PVDF film with either the continuous or reversely connected electrode integrated, Fig. 2 (c), and then cyclically stretched. The continuous electrode pattern has an effective area of 43 mm $\times$ 6 mm, and the inter-segment connection electrode has an effective surface of 9 mm $\times$ 6 mm in a single, quarter wavelength, unit. The experimental results, Fig. 2(d), substantially validated the efficiency of the inter-segment connection design, with a resulting 1.63 V generated voltage compared with 0.63 V generated voltage by the continuous electrode pattern under a given frequency of 10 Hz and a tensile strain of 10%. As seen in Fig. 2(d), the output voltage from both inter-segment and continuous electrode designs are not sine-shaped [Figs. S5(a) and S5(c)]. This is due to the relation between the global applied strain and local strain on the strip is not linear [Fig. S5(b)].

By using the optimized electrode design, the electric performance of the proposed sensor is explored under dynamic tests with controlled frequency excitation and strain ranges. Figure 3(a) shows the output voltage time histories at 10 Hz and tensile strain range between 2% and 10%. As shown in Fig. 3(b), the voltage increases linearly with applied strain. The output voltage time series at constant 1% tensile strain and frequency range from 3 Hz to 24 Hz are shown in Fig. 3(c). In this case also, the voltage output shows an almost linear dependency to the frequency increase under the fixed strain.

In conclusion, a stretchable piezoelectric sensor system with enhanced piezoelectric performance and high stretchability was obtained by introducing Kirigami patterns into a thin PVDF film with a PET film as the substrate, and an inter-segment electrode design to avoid charge cancellation and improve the piezoelectric generator effect. Experimental tests validated the significant improvement in voltage output with the adopted electrode pattern. Moreover, the Kirigami technique vastly extends the strain range of the sensor, while the piezoelectric performance remains stable. Dynamic tests under variable frequencies and strains also validated the efficiency and robustness of the sensing performance. The high stretchability and excellent piezoelectric operation of this Kirigami based piezoelectric sensor suggests its high suitability for implantable, self-powered biomedical devices and sensor systems.

See supplementary material for the Kirigami based piezoelectric sensor preparations, finite-element modelling, and characterization.

This work was supported by the Engineering and Physical Sciences Research Council through the EPSRC Centre for Doctoral Training in Advanced Composites for Innovation and Science (Grant No. EP/L016028/1). R. Sun acknowledges the support from the China Scholarship Council. J. Rossiter is supported by EPSRC Grant Nos. EP/M020460/1 and EP/M026388/1 and the Royal Academy of Engineering under the Chair in Emerging Technologies scheme. Data are available at the University of Bristol data repository, data.bris, at https://doi.org/10.5523/bris.ra5e2tx5hui528ykj8fmssl6i.

[1]Y. Cho, J. B. Park, B.-S. Kim, J. Lee, W.-K. Hong, I.-K. Park, J. E. Jang, J. I. Sohn, S. N. Cha, and J. M. Kim, Nano Energy **16**, 524 (2015).
[2]M. A. Parvez Mahmud, N. Huda, S. H. Farjana, M. Asadnia, and C. Lang, Adv. Energy Mater. **8**(2), 1701210 (2017).

[3]Q. Zheng, B. Shi, Z. Li, and Z. L. Wang, Adv. Sci. **4**(7), 1700029 (2017).
[4]Y. Hu and Z. L. Wang, Nano Energy **14**, 3 (2015).
[5]C. Dagdeviren, B. D. Yang, Y. Su, P. L. Tran, P. Joe, E. Anderson, J. Xia, V. Doraiswamy, B. Dehdashti, X. Feng, B. Lu, R. Poston, Z. Khalpey, R. Ghaffari, Y. Huang, M. J. Slepian, and J. A. Rogers, Proc. Natl. Acad. Sci. **111**(5), 1927 (2014).
[6]K.-I. Park, J. H. Son, G.-T. Hwang, C. K. Jeong, J. Ryu, M. Koo, I. Choi, S. H. Lee, M. Byun, Z. L. Wang, and K. J. Lee, Adv. Mater. **26**(16), 2514 (2014).
[7]Z. L. Wang and J. Song, Science **312**(5771), 242 (2006).
[8]S. Xu, Y. Qin, C. Xu, Y. Wei, R. Yang, and Z. L. Wang, Nat. Nanotechnol. **5**, 366 (2010).
[9]Y. Yu, H. Sun, H. Orbay, F. Chen, C. G. England, W. Cai, and X. Wang, Nano Energy **27**, 275 (2016).
[10]J. Fu, Y. Hou, M. Zheng, Q. Wei, M. Zhu, and H. Yan, ACS Appl. Mater. Interfaces **7**(44), 24480 (2015).
[11]A. Lund, C. Gustafsson, H. Bertilsson, and R. W. Rychwalski, Compos. Sci. Technol. **71**(2), 222 (2011).
[12]L. Yang, H. Ji, K. Zhu, J. Wang, and J. Qiu, Compos. Sci. Technol. **123**, 259 (2016).
[13]Y. Mao, P. Zhao, G. McConohy, H. Yang, Y. Tong, and X. Wang, Adv. Energy Mater. **4**(7), 1301624 (2014).
[14]L. Xu, T. C. Shyu, and N. A. Kotov, ACS Nano **11**(8), 7587 (2017).
[15]S. J. P. Callens and A. A. Zadpoor, Mater. Today **21**(3), 241 (2018).
[16]Y. Tang and J. Yin, Extreme Mech. Lett. **12**, 77 (2017).
[17]Y. Tang, G. Lin, L. Han, S. Qiu, S. Yang, and J. Yin, Adv. Mater. **27**(44), 7181 (2015).
[18]Y. Cho, J.-H. Shin, A. Costa, T. A. Kim, V. Kunin, J. Li, S. Y. Lee, S. Yang, H. N. Han, I.-S. Choi, and D. J. Srolovitz, Proc. Natl. Acad. Sci. **111**(49), 17390 (2014).
[19]A. Rafsanjani and K. Bertoldi, Phys. Rev. Lett. **118**(8), 084301 (2017).
[20]M. Isobe and K. Okumura, Sci. Rep. **6**, 24758 (2016).
[21]T. C. Shyu, P. F. Damasceno, P. M. Dodd, A. Lamoureux, L. Xu, M. Shlian, M. Shtein, S. C. Glotzer, and N. A. Kotov, Nat. Mater. **14**(8), 785 (2015).
[22]T. Han, F. Scarpa, and N. L. Allan, Thin Solid Films **632**, 35 (2017).
[23]A. Lamoureux, K. Lee, M. Shlian, S. R. Forrest, and M. Shtein, Nat. Commun. **6**, 8092 (2015).
[24]Z. Wang, L. Zhang, S. Duan, H. Jiang, J. Shen, and C. Li, J. Mater. Chem. C **5**(34), 8714 (2017).
[25]J. Lyu, M. D. Hammig, L. Liu, L. Xu, H. Chi, C. Uher, T. Li, and N. A. Kotov, Appl. Phys. Lett. **111**(16), 161901 (2017).
[26]M. K. Blees, A. W. Barnard, P. A. Rose, S. P. Roberts, K. L. McGill, P. Y. Huang, A. R. Ruyack, J. W. Kevek, B. Kobrin, D. A. Muller, and P. L. McEuen, Nature **524**(7564), 204 (2015).
[27]M. A. Dias, M. P. McCarron, D. Rayneau-Kirkhope, P. Z. Hanakata, D. K. Campbell, H. S. Park, and D. P. Holmes, Soft Matter **13**(48), 9087 (2017).
[28]Z. Song, X. Wang, C. Lv, Y. An, M. Liang, T. Ma, D. He, Y.-J. Zheng, S.-Q. Huang, H. Yu, and H. Jiang, Sci. Rep. **5**, 10988 (2015).
[29]H. Guo, M.-H. Yeh, Y.-C. Lai, Y. Zi, C. Wu, Z. Wen, C. Hu, and Z. L. Wang, ACS Nano **10**(11), 10580 (2016).
[30]W. Wang, C. Li, H. Rodrigue, F. Yuan, M.-W. Han, M. Cho, and S.-H. Ahn, Adv. Funct. Mater. **27**(7), 1604214 (2017).
[31]Y. Tang, G. Lin, S. Yang, Y. K. Yi, R. D. Kamien, and J. Yin, Adv. Mater. **29**(10), 1604262 (2016).
[32]Y. Morikawa, S. Yamagiwa, H. Sawahata, R. Numano, K. Koida, M. Ishida, and T. Kawano, Adv. Healthc. Mater. **7**(3) (2018).
[33]J. M. Rossiter, B. L. Stoimenov, and T. Mukai, Proc. SPIE **6524**, 65241B (2007).